Original Article

Impact of Remdesivir on the kidney and Potential Protective Capacity of Granulocyte-Colony Stimulating Factor Versus Bone Marrow Mesenchymal Stem Cells in Adult Male Albino Rats

Hala El-Haroun[1], Manar Ali Bashandy[2] and Mona Soliman[1]

[1]Department of Histology, [2]Department of Anatomy and Embryology, Faculty of Medicine, Menoufia University, Egypt.

ABSTRACT

Background: Remdesivir is a novel broad spectrum antiviral drug previously used to treat Ebola. It is a pro-drug nucleoside with antiviral activity that is opposed to SARS-CoV-2 and coronavirus.

Aim: Current research was planned to evaluate and compare the potential ameliorative impact of the hematopoietic-stem-cell mobilized by the granulocyte colony-stimulating factor (G-CSF) versus BM-MSC on the effect of novel antiviral remdesivir on the kidney.

Materials and Methods: Rats divided into four groups: control group, Remdesivir treated group (20 mg/kg/day IV on the first day followed by 10 mg/kg/day for 6 days), Remdesivir + BM-MSCs group ($3x10^6$ cells/ml of PKH26 labelled MSC) and Remedesivir+ Filgrastim group (70 µg/kg/day/5 days). At the end of the experiment, animals were anaesthetized and sacrificed. Both animal kidneys were excised for histological, immunohistochemistry, and electron microscopy studies. Biochemical and morphometric assessments had been performed.

Results: Remdesivir caused distortion and degeneration of both the glomeruli and the renal tubules associated with Bowman's space widening. It greatly increased the deposition of collagen and enhanced the expression of caspase 3, IL-6, and TGF-β1. Ultrastructure changes were observed in the form of thickening of glomerular basement membrane, dilated basal plasma membrane infoldings of tubular epithelium and mitochondrial degeneration. Biochemically, decreased antioxidant enzymes, reduced glutathione (GSH), superoxide dismutase (SOD), and catalase (CAT) with increased serum urea and creatinine were also recorded. Both BM-MSCs and G-CSF improved histological structure and function of the kidney.

Conclusion: Prescribing drugs such as remdesivir should be carried out with severe care. BM-MSCs and G-CSF are an efficient and ideal option to protect patients from irreversible kidney damage.

Received: 30 January 2021, **Accepted:** 20 March 2021

Key Words: BM-MSCs, G-CSF, remdesivir.

Corresponding Author: Hala El-Haroun, PhD, Department of Histology, Faculty of Medicine, Menoufia University, Egypt, **Tel.**: +2 03 582 7472, **E-mail:** elharoun@yahoo.com

ISSN: 1110-0559, Vol. 45, No.2

INTRODUCTION

Severe acute respiratory syndrome coronavirus 2 (SARS-CoV-2) is a cause for a contagious diseases called COVID-19. It is the cause of a rising number of deaths globally, as no potent medication is available[1]. Remdesivir (GS-5734) is a wide-spectrum antiviral medication first identified in 2015 and previously used as an effective treatment for the Ebola virus[2]. It is a nucleoside pro-drug with in *vitro* antiviral activity in addition to bat SARS-CoV-2 and coronavirus, as well as human airway epithelium culture and improving disease severity in experimental mouse model studies[3,4]. It is assumed to be attributable to inhibition of viral RNA transcription and replication as demonstrated in cell culture supporting its effect[5,6].

The molecular weight of Remdesivir is 602.6 g/mol and the solubility in water is low. It is typically given by intravenous route at a dosage (200 mg once and then a total of 100 mg daily) for 5-10 days in patients of body weight larger than 40 kg. Remdesivir and its active metabolites are mainly excreted by the kidney (74 %). It has a short plasma half-life of 1-2 hours, while its active metabolite (remdesivir triphosphate) has a long half-life of 20-25 hours, leading to broad dissemination to many body tissues[3]. Significant concerns have been raised regard to relative drug toxicity in patients with renal disease due to both drug action and carrier deposition (sulfobutyl ether-β-cycodextrin SBECD)[7].

It has been successfully used for the management of one case of SARS-CoV-2 pneumonia in the USA[4]. In addition, two case report studies and a multinational treatment trial were correlated with the beneficial impact of Remdesivir on serious COVID-19 pneumonia cases[8,9] and also a randomized clinical trial to test its effect[10].

Some researchers indicated that the most common adverse reactions to remdesivir were increased liver enzymes and total bilirubin reported by Grein and his colleagues[8]. However, acute kidney injury, rash, and drug discontinuation due to intolerance have been recorded[1].

 DOI: 10.21608/ejh.2021.60527.1426

Previous research in rhesus monkeys model recorded kidney damage at doses higher than those used in corona patients[7]. Animal studies have hypothesized that sulfobutylether-β-cyclodextrin (SBECD) accumulation contributes to obstruction of renal tubules and liver necrosis when remdesivir is used[11].

Bone marrow mesenchymal stem cells (BM-MSCs) are able of self-replication, hematopoietic support and multi-lineage differentiation. They also have tissue renovation, anti-inflammatory and immune-modulatory roles[12]. BM-MSCs are safe therapeutic choice since they are isolated from the bone marrow of the same patient[13]. They have numerous advantages as they can be stored safely for a long period of time without any reaction to their allogeneic transplantation[14]. Experimental studies have shown that BM-MSCs have been proven to be beneficial for kidney injury, myocardial infarction, lung, corneal, spinal cord, and brain injury[15,16]. In animal model studies, enhanced renal function and structure was achieved following BM-MSC infusion to treat acute renal injury[17,18]. In addition, Yen and his colleagues[19] researched the effect of male BM-MSCs transplanted to female mice as a therapeutic procedure for the treatment of renal tubular injury. Approximately 4 % of the tubular cells were found to have a positive Y-chromosome suggesting that male BM-MSc plays a novel rule in renal regeneration. Moreover, the process of therapeutic action of BM-MSCs in renal remediation is thought to be due to endocrine and/or paracrine pathways by release of cytokines and trophic growth factors as vascular endothelial growth factor (VEGF), insulin like growth factor-1 (IGF-1) and fibroblast growth factor[20] by modulate ting immune response, inducing repair and stimulating proliferation[21]. Previous studies have indicated that in laboratory rodents, novel BM-MSCs may be utilized to prevent the release of pro-inflammatory cytokines through renal regenerative and protective effects[22].

Recombinant human granulocyte-colony stimulating factor (G-CSF) is considered to be a promising and well tolerated therapeutic option[23]. G-CSF has developed a variety of innovative clinical applications as a valuable therapeutic alternative for the recovery of damaged organs. Previous research explored the therapeutic efficacy of G-CSF on organ regeneration in myocardial infarction but was still controversial[24]. Other laboratory findings have demonstrated that the therapeutic effect of G-CSF was efficient in case of induced acute renal failure in mouse models contributing to improved renal function and renal damage relative to control mice with the same renal injury[25,26].

Researchers[27, 28] have reported that G-CSF promotes specific and temporary raise in circulating neutrophils by enhancing bone marrow formation. As a consequence, G-CSF has a therapeutic role in neutropenic patients collecting the progenitor cells required for hemopoietic stem cell transplantation (HSCs).

Based on previous findings on the therapeutic impact of BM-MSCs in renal injury and the regenerative effect of G-CSF in injured organs, the current research was planned to evaluate the probable ameliorative effect of G-CSF compared to BM-MSCs on acute renal injury caused by a novel antiviral drug; Remdesivir using histological, immunohistochemical, ultrastructure and biochemical assessments.

MATERIALS AND METHODS

Animals

Fifty-seven adult male albino rats (12 weeks old) with an average weight of 180-220 grams have been used in the experiment. Animals were supplied from the animal house at the Faculty of Medicine, Menoufia University, and one week before the start of the experiment to be acclimatized under laboratory conditions. Rats were housed in safe standard environmental conditions at room temperature with unrestricted diet and water supplies.

Chemicals

Remdesivir were obtained from EVA pharma (Egypt) in the form of vial 100mg/ 20 ml.

G-CSF- Filgrastim is Recombinant human granulocyte-colony stimulating factor 300 µg/ml (liquid for S.C or I.V injection) was purchased from SEDICO Pharmaceuticals Company (Egypt).

Bone marrow derived- MSCs (BMSCs) labeled with PKH67 (Green Fluorescent Cell Linker) were supplied by the unit of stem cell research at the Biochemistry department of the Faculty of Medicine, Cairo University, Egypt. Kidney tissue was studied with a fluorescent microscope (Olympus BX50F4, No. 7M03285, Tokyo, Japan) to identify and track PKH67-stained cells (Figures 1A,1B).

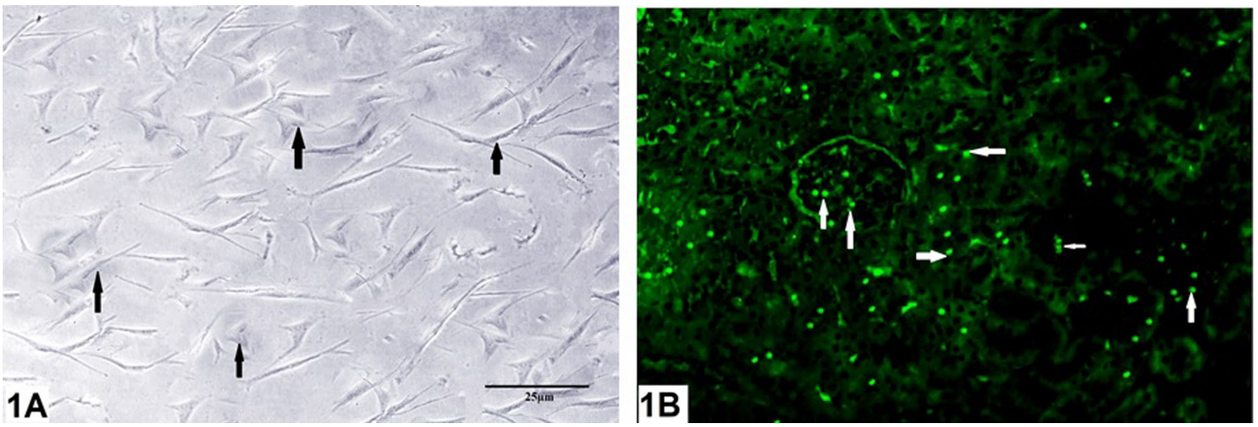

Fig. 1(A): 10-day culture, inverted microscope micrograph of bone marrow mesenchymal stem cells (BMSCs). The cells are spindle-shaped cells.
(B): Remdesivir and Stem cell-treated renal cortex display PKH67 labelled cells appearing as bright spots inside the tubules and corpuscles. Bar scale=25; fluorescent microscope.

Experimental procedure

The rats have been randomly divided into four groups:

Group I (control group) (n=18 rats) was divided into 3 subgroups included 6 animals for each:

Group Ia: the animals in this group have remained untreated.

Group Ib: (BMSCs treated group): Each rat of this group received 0.5 ml of PKH26 labelled MSC suspension in BPS ($3x10^6$ cells/ml) for two consecutive days via the tail vein[29].

Group Ic: Each rat in this group received Filgrastim (70 µg/kg/day SC for 5 days)[30].

Group II (Remedesivir treated group) (n=13 rats): Rats got 20 mg/kg/day IV on the first day followed by 10 mg/kg/day for 6 days according to Thakare *et al*.[31]. Dose has been converted from human to animal according to Shin *et al*.[32].

Group III (Remedesivir and BMSCs treated group) (n=13 rats): 1 ml of PKH26-labelled MSC suspension in BPS was administered to rats on day 1 following administration of remediesivir for two consecutive days ($3x10^6$ cells/ml) IV via tail vein[29].

Group IV (Remedesivir and Filgrastim treated group) (n=13 rats): animals received Filgrastim (70 µg/kg/day) two hours after remediesivir injection for 5 days.

After 5 days of the start of the experiment, 3 animals of each group were sacrificed and Kidney samples were obtained, processed and immunostained with anti-CD34 antibody to evaluate the mobilization and homing of HSCs in the kidneys.

On the 21st day of the beginning of the experiment, the remaining animals were weighed and then sacrificed.

Biochemical assessment

1. Urea and creatinine: Collected blood samples from the animals were centrifuged, and the plasma was isolated to estimate spectrophotometric levels of urea and creatinine using assay kits. (Bio Merieux, Marcy-l'Etoile, France). This was done in central lab, Faculty of Medicine, Menoufia University.
2. Renal oxidative stress markers: For the determination of antioxidant enzymes, kidney tissue was extracted and homogenised in potassium phosphate buffer solution (50 mM, pH 7.5) using a Potter Elvehiem homogenizer to achieve 10% homogeneity. The mixture have been centrifuged at 1500 g for 10 min at 4°C; supernatant has been retrieved, put on ice and subsequently included in measurement of reduced glutathione (GSH), superoxide dismutase (SOD), catalase (CAT) and Malondialdehyde (MDA). Reduced (GSH) in the kidney were measured by a spectrophotometric detection method[33]. The activity of SOD was calculated in accordance with the procedure of Jurczuk *et al*,[34] using spectrophotometer. CAT activity was assayed according to Jurczuk *et al*,[34]. Catalase activity was determined from the rate of decomposition of H_2O_2. MDA, as an indicator for oxidative damage was measured colorimetrically in kidney homogenate according to the method of Jurczuk *et al*,[34].

Light microscopic studies

Histological study

Kidney specimens from each animal were fixed in 10 % formol saline, dehydrated, cleared and embedded in paraffin wax. For standard histological analysis of the general architecture of Kidney, five µm thickened sections were cut and stained with haematoxylin and eosin (Hx&E) and Mallory's Trichrome stain for identification of collagen fibers[35].

Immunohistochemical study

Anti-CD34 antibody immunostaining: the primary antibody used was the mouse monoclonal anti-CD34

antibody (Dako, Glostrup, Denmark), to display HSCs. The cytoplasmic brown reaction indicates positive cells[36].

Anti-caspase-3 antibody immunostaining

The primary antibody used to assess apoptosis was the ready-to-use rabbit polyclonal antibody (Thermo Scientific Laboratories, Neo Markers, and Waltham, Massachusetts, USA). A cytoplasmic brown reaction was exhibited by positive cells[36].

Transforming growth facor- β1 (TGF-β1) immunostaining

Rabbit anti TGF-β1 (Santa-Cruz Biotechnology, Santa Cruz, CA), was the primary polyclonal antibody used (diluted 1:100 with PBS). Cytoplasmic brown in colour was the cellular site of the reaction[37].

Interlukin-6 (IL-6)

Immunostain IL-6 mouse monoclonal antibody (Sc-130326) (Santa Cruz biotechnology company, ABC staining system: Sc-2017) was applied. Sections were incubated with primary antibodies for overnight at room temperature then incubated with goat anti-mouse biotinylated IgG (no. B0529; Sigma[38].

Positive control CD34: placenta

Positive control TGF-B1: Spleen

Positive control IL-6: Skin

Positive control caspase 3: normal lymphoid tissue.

Negative Control: Omit primary antibody.

The sections were counterstained with hematoxylin[38,39].

II- Electron Microscopic study

Tiny pieces (1mm) of the kidney were rapidly sliced and directly fixed to 3% of glutaraldehyde buffered with 0.1 mol/L PBS at pH 7.4 for 3 hours at 4°C and fixed to 1 % of osmium tetroxide in the same buffer for 2 hours at 4°C. The tissue was then dehydrated in ascending grades of alcohol and embedded in the epoxy resin. Ultrathin sections were stained with uranyl acetate and lead citrate to be analysed and captured using a transmission electron microscope (JEOL, JEM-2100, Tokyo, Japan)[40] at the Faculty of Science, Alexandria University, Alexandria, Egypt.

Morphometrical study

For quantitative evaluation, ten different separate fields from each section were measured employing a Leica DML B2/11888111 microscope supplied with a Leica DFC450 camera. The measured variance was estimated using the software version K1.45 of Image J. The measured data were undertaken using H&E, Mallory's Trichrome and immunohistochemical sections. For quantitative evaluation, the following illustrated parameters were calculated:

- Diameter of Bowman's space. (x 400).
- Diameter of renal corpuscle. (x 400).
- Mean area percentage of collagen fibers with sections stained with Mallory's Trichrome (x 400).
- Caspase 3 immunopostive intensity (x400).
- IL6 immunopositive intensity (x 400).
- TGF-β1immunopositive intensity (x 400).

Statistical analysis: The results of different groups were expressed as mean±SD. In order to determine statistical significance, the different parameters obtained from different groups were compared using both the one-way variance analysis (ANOVA) and Bonferroni's post-hoc test. Data were assessed at $P < 0.001$ as statistically significant. The results were reported or graphically plotted in tables[41].

RESULTS

The animals were in good general condition and displayed normal conduct, behaviour, and appetite. No considerable difference in animal body weight was found in all classes. The 3 subgroups of control group were similar in their results. Compared to other groups, there was a marked increase in renal weight in the remdesivir treated group (Figures 2A,2B).

Biochemical results

In the control group, there was no significant difference between the subgroups (Ia, Ib. Ic). Remdesivir treated animals displayed a significant increase in serum urea and creatinine ($P < 0.001$) relative to the control group as well as the remdesivir and BMSC and G-CSF treated groups (Figures 2C,2D). Treatment of remdesivir showed significant reduction in GSH relative to the control group and that treated with remdesivir and BMSC and G-CSF (Figure 3A). The MDA level showed non-significant differences between all groups (Figure 3B). The activity of the antioxidant enzymes catalase (CAT) and enzyme (SOD) in the remdesivir-treated group has also shown a significant decrease ($P < 0.001$). In contrast to remdesivir-treated rats, treatment with either BMSCs or G-CSF induced a significant increase ($P<0.001$) in antioxidant enzymes (SOD, CAT) (Figures 3C,3D). All parameters were set in (Table 1).

Light microscopic results

Hematoxylin and Eosin-stained sections of the all control subgroup (Ia, Ib, Ic) showed that the renal cortex composed of Malpighian renal corpuscle (MRC) that appeared as spherical structures of glomerular capillary tuft enveloped by the Bowman's membrane that lined with simple squamous epithelium enclosing a narrow space of Bowman (subcapsular space). The proximal convoluted tubules (PCT) were lined with cuboidal cells with rounded basal nuclei, deep acidophilic cytoplasm, apical clear brush borders and narrow lumen. Less acidophilic cytoplasm

and non-clear brush border lined distal convoluted tubules (DCT), which had a wider lumen, cubic cells with rounded central nuclei (Figures 4A,4B).

Sections of the group treated with remdesivir (group II) exhibited significant disruption of the histology of the renal cortex. The glomeruli seemed to be swollen, fragmented, and degenerated with significant increase in diameter (P<0.001) (Figure 4I) The glomerular capillaries lined with small pyknotic nuclei that were darkly stained (Figures 4C,4D,4E,4F). Other glomeruli had congested capillaries (Figure 4F). The parietal layer of Bowman's capsule seemed to be interrupted with significant widening of Bowman's space (P<0.001) (Figures 4C,4D,4J). Dilated Renal tubules having acidophilic cast within their lumen, seemed to be distorted with epithelial linings having nuclei with variable degrees of degeneration (pyknosis and karyolysis) (Figures 4C,4D,4E). There was degeneration of the renal interstitium leaving wide spaces in between renal tubules (Figure 4E). Peritubular capillaries tended to be congested and dilated. Some of them had an obvious thick wall (Figure 4F).

Sections of BM-MSCs and remdesivir treated renal cortex group (Group III) displayed marked improvements in the remdesivir-induced changes the renal cortex. Nearly normal renal glomeruli appeared surrounded by Bowman's capsule. Few glomerular capillaries were still dilated and congested with almost normal renal tubules and renal interstitium (Figure 4G).

Reconstruction of renal glomeruli was seen in the renal cortex within the sections of the GCSF and remdesivir-treated group (Group IV). However, some glomerular capillaries have been slightly dilated. The space of Bowman seemed to be regular. Renal tubules tended to be more or less normal. Renal interstitium between renal tubules appeared to be normal (Figure 4H).

Mallory trichrome stained sections of the control group (I) in the renal cortex revealed a limited amount of collagen fiber in the renal interstitium like between the glomerular capillaries (Figure 5A). However, the amount of collagen fibres within the interstitium and between the glomerular capillaries in the renal cortex sections of the remdesivir-treated group (II) increased remarkably significantly (P<0.001) (Figures 5B,5E). Minimal amounts of collagen fibers in renal interstitium and in-between glomerular capillaries were identified in Group III (BM-MSCs and Remdesivir) like those in the control group (Figure 5C). Group IV (G-CSF and remdesivir) registered a small amount of collagen fiber in the renal interstitium and between the glomerular capillaries (Figure 5D).

CD34 immune marker expression: on day 5 cortical renal sections of the control group (I) found positive immune reaction in endothelial cells and no immunoreactive hematopoietic stem cells were found (Figure 6A). Group II (remdesivir) demonstrated minimal immunopositive reactivity in glomerular and endothelial cells (Figure 6B). A variety of immunoreactive hematopoietic stem cells was present in Group III renal glomeruli and tubular epithelium (Remdesivir+ BM-MSCs) (Figure 6C). In group IV (Remdesivir+G-CSF), many immunoreactive cells have been shown in both glomerular and tubular epithelium as well as endothelial cells (Figure 6D).

Caspase-3 immunomarker expression: The renal cortex sections of the control group (I) were negative (Figure 6E). Group II (Remdesivir) demonstrated a significant strong positive immune-histochemical cytoplasmic response within the epithelial tubular and a moderate glomerular positive response to caspase-3 (Figures 6F,6I). Negative cytoplasmic reactions were observed in glomerular and tubular epithelium in group III (BM-MSCs+ Remdesivir) (Figure 6G) and group IV (G-CSF +remdesivir) (Figure 6H).

TGF-β1 immune marker expression within the renal cortex sections of the control group (I) was negligible (Figure 7A). Group II (treated with remdesivir) displayed a significant (P< 0.001) strong positive immune-histochemical cytoplasmic response within the glomerular and tubular epithelium to TGF-β1 (Figures 7B,7I). A negative cytoplasmic reaction of TGF-β1 inside the glomerular and tubular epithelium was observed in group III (stem cells and remdesivir) close to that of the control group (Figure 7C). Similarly, Group IV (G-CSF and remdesivir) exhibited the same negative cytoplasmic reaction to TGF-β1 inside the glomerular and tubular epithelium (Figure 7D).

IL-6 immune marker expression within sections of the renal cortex of the control group (I) were negative (Figure 7E). Group II (treated with remdesivir) demonstrated a significant strong positive (P< 0.001) immune-histochemical cytoplasmic reaction within tubular epithelial and a moderate glomerular positive reaction to IL-6 (Figures 7F,7J). There was a negative cytoplasmic reaction of IL-6 within the glomerular and tubular epithelium group III (BM-MSCs and remdesivir group) close to that of the control group (Figure 7G). Group IV (G-CSF and remdesivir) demonstrated negative cytoplasmic IL-6 reactions inside the glomerular and tubular epithelium (Figure 7H).

Electron Microscopic Results

Renal cortex of control Group (Group I) exhibited renal glomeruli lined with podocytes having euchromatic nuclei. They had primary and secondary processes wrapping glomerular capillary. Secondary processes (feet) were separated by filtration slits covered by diaphragm. The glomerular capillaries had euchromatic nucleus with intact, uniform basement membrane. The glomerular basement membrane was smooth having regular diameter (Figure 8A).

Proximal convoluted tubule lined with epithelial cells resting on the clear basement membrane with central euchromatic nuclei, multiple basal membrane in-folding and long slim packed luminal microvilli. Their cytoplasm

showed multiple longitudinally oriented mitochondria and lysosomes (Figure 8B).

Distal convoluted tubule lining cells were resting on clear basement membrane having centrally located euchromatic nucleus, apical scarce short microvilli, basal membrane in-folding. Their cytoplasm had multiple mitochondria RER, free ribosomes and lysosomes (Figure 8C).

However, renal cortex of Remdesivir treated group (II) displayed irregular marked thickening of glomerular basement membrane. Podocytes had heterochromatic nuclei. Fusion and broadening of secondary foot processes on basement membrane of glomerular capillary with loss of slit diaphragms in-between were observed (Figure 8D).

Proximal convoluted tubules lining cells had rarified cytoplasm with multiple vacuoles and lysosomes. Disturbed luminal surface with multiple vacuoles and dilated basal plasma membrane in-folding with degenerated mitochondria were recorded (Figure 8E).

There were heterochromatic nuclei in the distal convoluted tubules lining cells. The basal plasma membrane displayed dilated infoldings of the basal plasma membrane with degenerated mitochondria and loss of apical plasma membrane micro-projection (Figure 8F).

The BM-MSCs and remdesivir treated group (III) displayed renal glomeruli showing podocytes with indented heterochromatic nucleus with almost typical secondary processes (feet) wrapping clear thin basement membrane with standard diameter (Figure 8G).

Proximal convoluted tubules lining cells resting on clear basement membrane had central euchromatic nucleus. The membrane exhibited multiple basal plasma infoldings with multiple longitudinally oriented mitochondria, while luminal border had long slim packed microvilli. Their cytoplasm contained lysosomes, and few apically located vacuoles (Figure 8H).

Distal convoluted tubule cells resting on clear basement membrane had centrally located euchromatic nucleus with apical short microvilli. Their cytoplasm showed multiple longitudinally oriented mitochondria, lysosomes, RER, and free ribosomes with basal membrane infoldings (Figure 8I).

The GCSF and remdesivir treated group (IV) displayed renal glomeruli podocytes with heterochromatic nucleus and primary and secondary processes (feet) wrapping thin basement membrane of irregular diameter. The secondary processes are irregular in shape showing broadening and fusion in many sites (Figure 8J).

The cells lining of proximal convoluted tubules had euchromatic nuclei. The luminal surface had apical long microvilli. The cytoplasm had numerous mitochondria, lysosomes, normal rough endoplasmic reticulum, and focal lytic areas with apical vacuoles (Figure 8K).

Distal convoluted lining cells had central rounded euchromatic nucleus. The cytoplasm had nearly normal mitochondria. Dilated basal plasma membrane infoldings, multiple lytic areas within the cytoplasm and loss of apical luminal microvilli were recorded (Figure 8L).

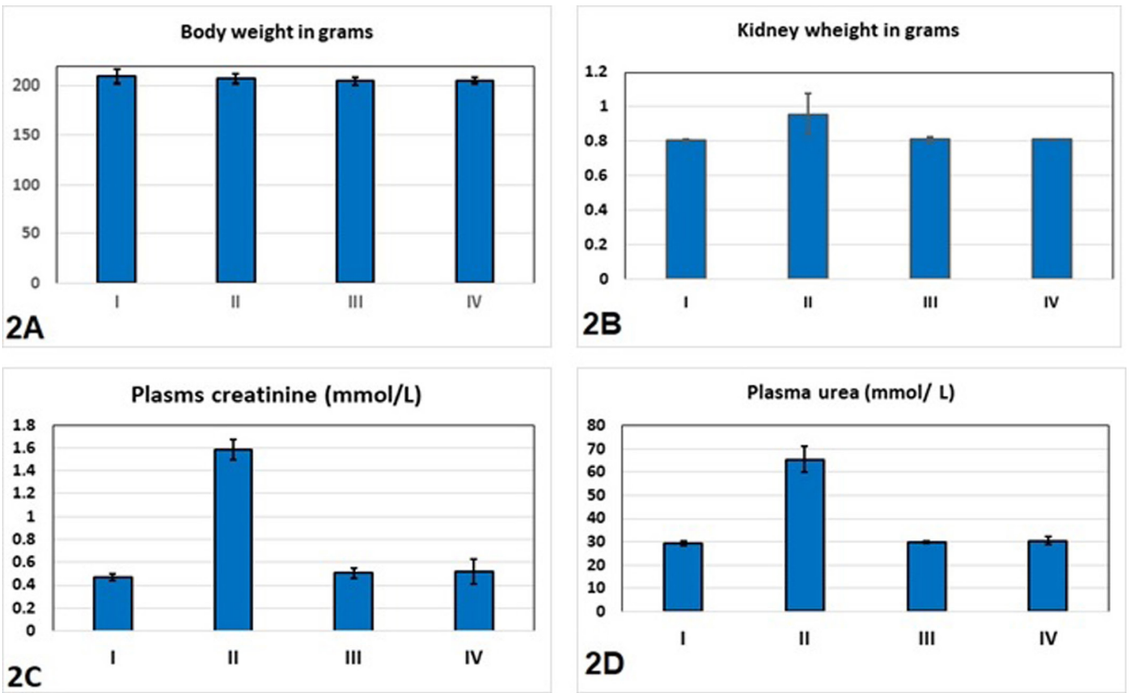

Fig. 2: (A) A histogram showing mean body weight in grams
(B) A histogram showing mean of kidney weight in grams
(C) A histogram showing mean of Plasma creatinine (mmol/L)
(D) A histogram showing mean of Plasma urea (mmol/ L)

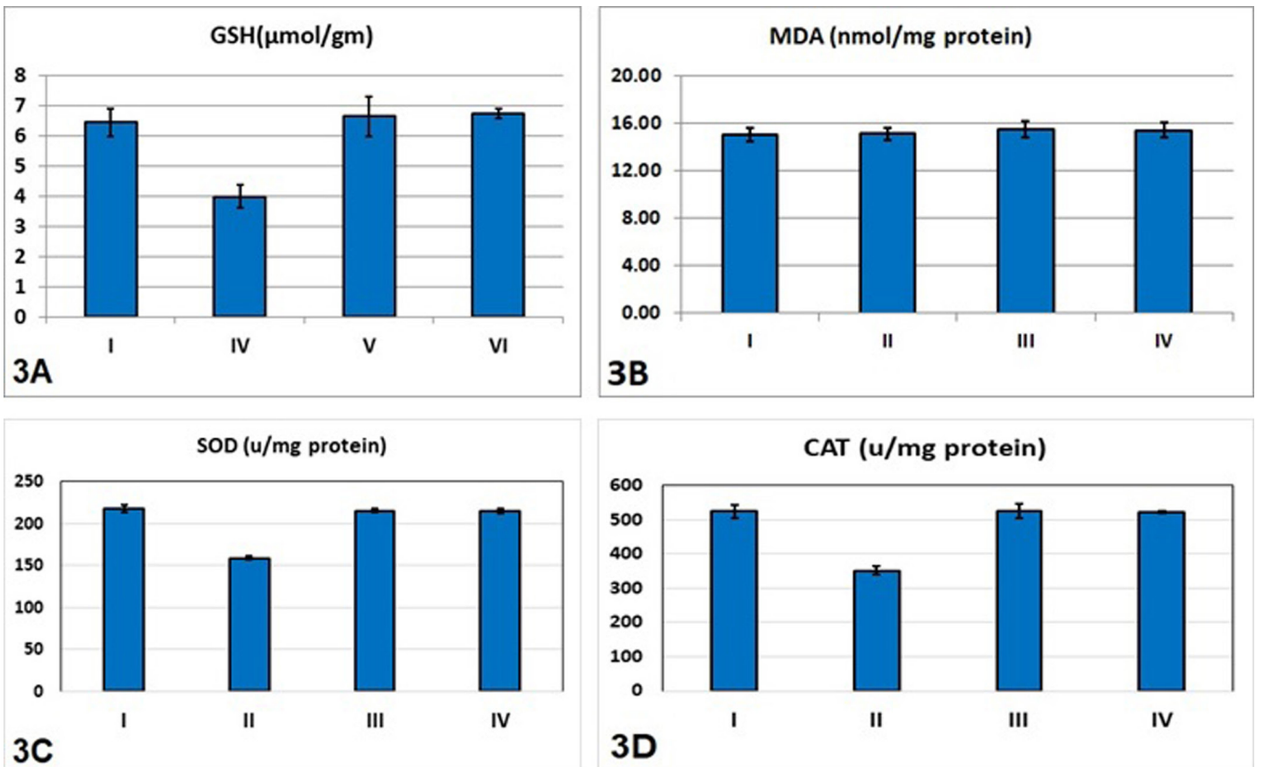

Fig. 3: The activity of the antioxidant enzymes:
(A) A histogram showing mean of reduced glutathione (GSH) (µmol/gm)
(B) A histogram showing mean of MDA (nmol/mg protein)
(C) A histogram showing mean of SOD (u/mg protein)
(D) A histogram showing mean of CAT (u/mg protein)

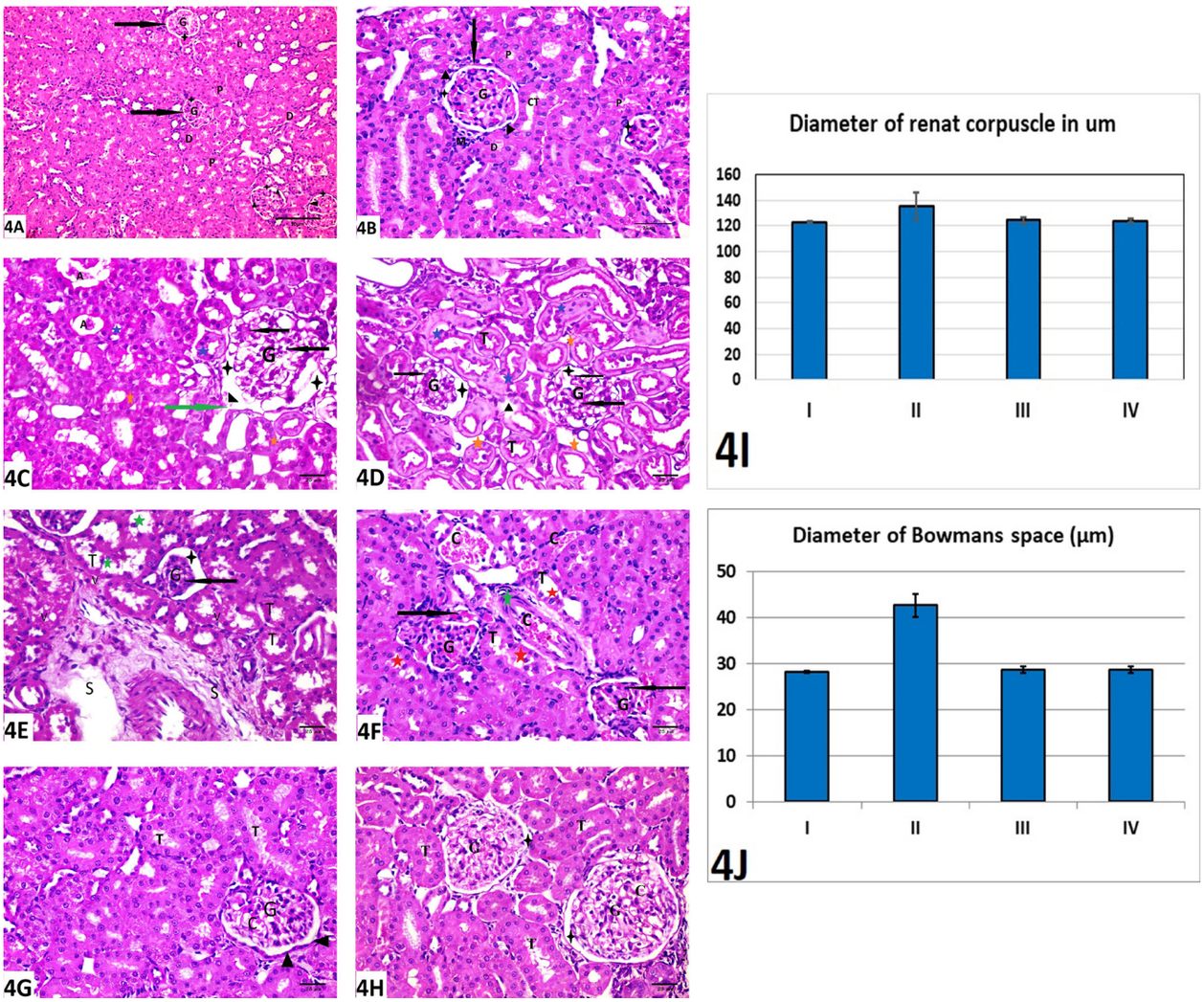

Fig. 4: H&E Sections of the renal cortex:
(A) Control group (I) exhibiting normal renal corpuscles (arrow) formed by a glomerular capillary tuft (G) encircled by a parietal layer of the Bowman capsule (arrowhead). Bowman's space (black star), proximal convoluted tubule (P) and distal convoluted tubule (D) are noticeable (x100)
(B): Control group (I) with a normal renal corpuscle (arrow) formed by a glomerular capillary tuft (G) surrounded by a parietal layer of Bowman capsule lined with a single layer of squamous cells (arrowhead). Clear Bowman's (subcapsular) space (black star) separates them. PCT (P) has a narrow lumen and its lining cells have a basal nucleus and a deeply acidophilic cytoplasm with an apical brush border. DCT (D) cells have large lumen and apical nuclei and less acidophilic cytoplasm. The collecting tubules (CT) are also visible. Note: the crowded nucleus in the wall of the distal tubules at the vascular pole of the renal corpuscle forming the macula densa (M) (x400).
(C): Remdesivir treated group (II) showing degenerated glomeruli (G) with widening of subcapsular space (black star) and discontinuation of the parietal layer of the Bowman capsule (arrowhead). Glomerular capillaries have small darkly stained nuclei (black arrow). Some of the tubules have dilated lumen with acidophilic casting (A) in their lumen and discontinued wall (green arrow). The epithelial lining shows varying degrees of degeneration (pyknosis (blue star) and Karyolysis (orange star) (x400).
(D): Remdesivir treated group (II) showing degenerated glomeruli (G) with widening of sub-capsular space (black star). Glomerular capillaries have small darkly stained (pyknotic) nuclei (back arrow). Renal tubules (T) appear distorted having dilated irregular lumen with discontinuity of some of their wall (arrowhead). Their epithelial lining has nuclei with variable degrees of degeneration (pyknosis (blue star) and karyolsis (orange star) (x400).
(E): Remdesivir treated group (II) showing degenerated glomeruli (G) having small darkly stained (pyknotic) nuclei (black arrow) lining the Glomerular capillaries. Bowman's space appeared widened (black star). Renal tubules (T) have dilated lumen with distorted epithelial lining. Some epithelial lining appears vacuolated (V). Other cells are detached within the lumen (green star). The renal interstitium appears degenerated having wide spaces(S) (x400).
(F): Remdesivir treated group (II) displaying segmented degenerated glomeruli (G). Glomerular capillaries have small darkly stained (pyknotic) nuclei (black arrow). Peritubular capillaries are dilated and congested (C). Some have apparent thick wall (green star). Notice: some renal tubules (T) have distorted epithelial lining with exfoliation of its cells within their lumen (red star) (x400).
(G): BM-MSCs and remedesivir treated group (III) showing nearly normal renal glomeruli (G) surrounded by normal parietal layer of Bowman's capsule lined with squamous cells (arrowhead). The few glomerular capillaries are still dilated and congested (C). Normal renal tubules (T) and renal interstitium (x400).
(H): GCSF and remedesivir-treated group (IV) demonstrating reconstruction of renal glomeruli (G) with normal Bowman's space (star). The glomerular capillaries are slightly dilated (C). Renal tubules (T) appear normal (x400).
(I) A histogram showing diameter of renal corpuscles in (µm).
(J) A histogram showing diameter of Bowmans space in (µm).

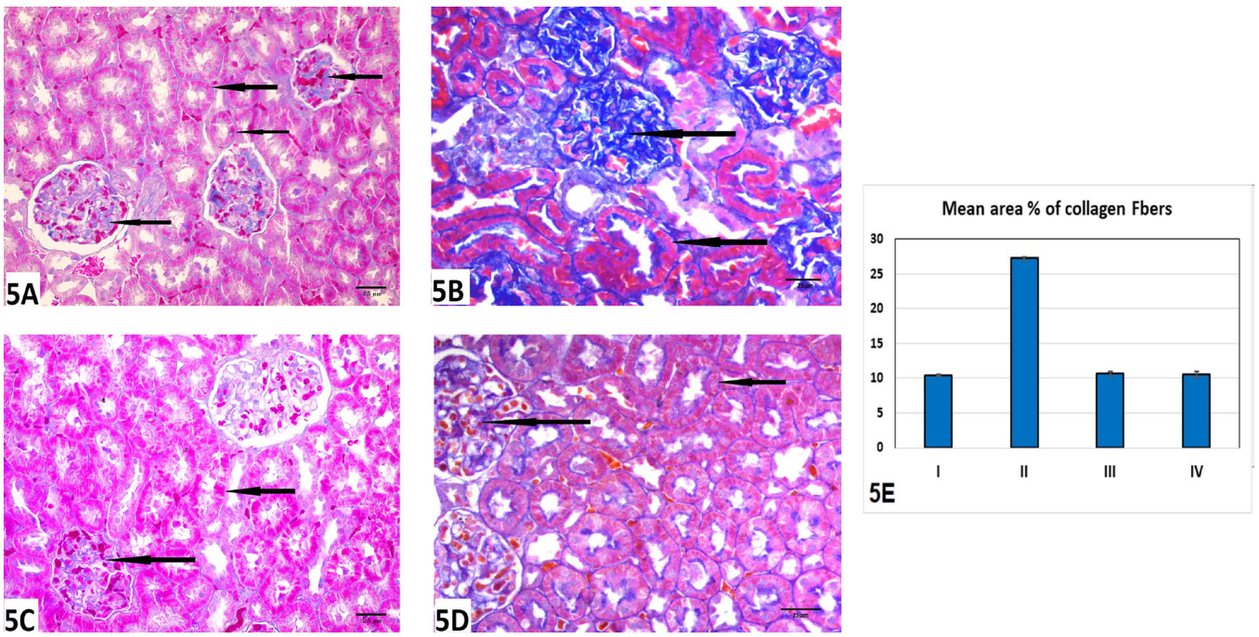

Fig. 5: (A-E): A section of renal cortex Mallory's trichrome (x400)
(A) Control group (I) demonstrating minimal amount of collagen fibers in the renal interstitium and in between glomerular capillaries(arrows).
(B): Remdesivir treated group (II) displaying an increase of the collagen fibers in the interstitium and in between glomerular capillaries (arrows).
(C): BM_MSCs and remediesivir treated group (III) displaying a slight amount of collagen fibers in the renal interstitium and between the glomerular capillaries (arrows).
(D): GCSF and the remdesivir-treated group (IV) reveals a small amount of collagen fibers in the renal interstitium and between the glomerular capillaries (arrows).
(E): A histogram showing mean area % of collagen.

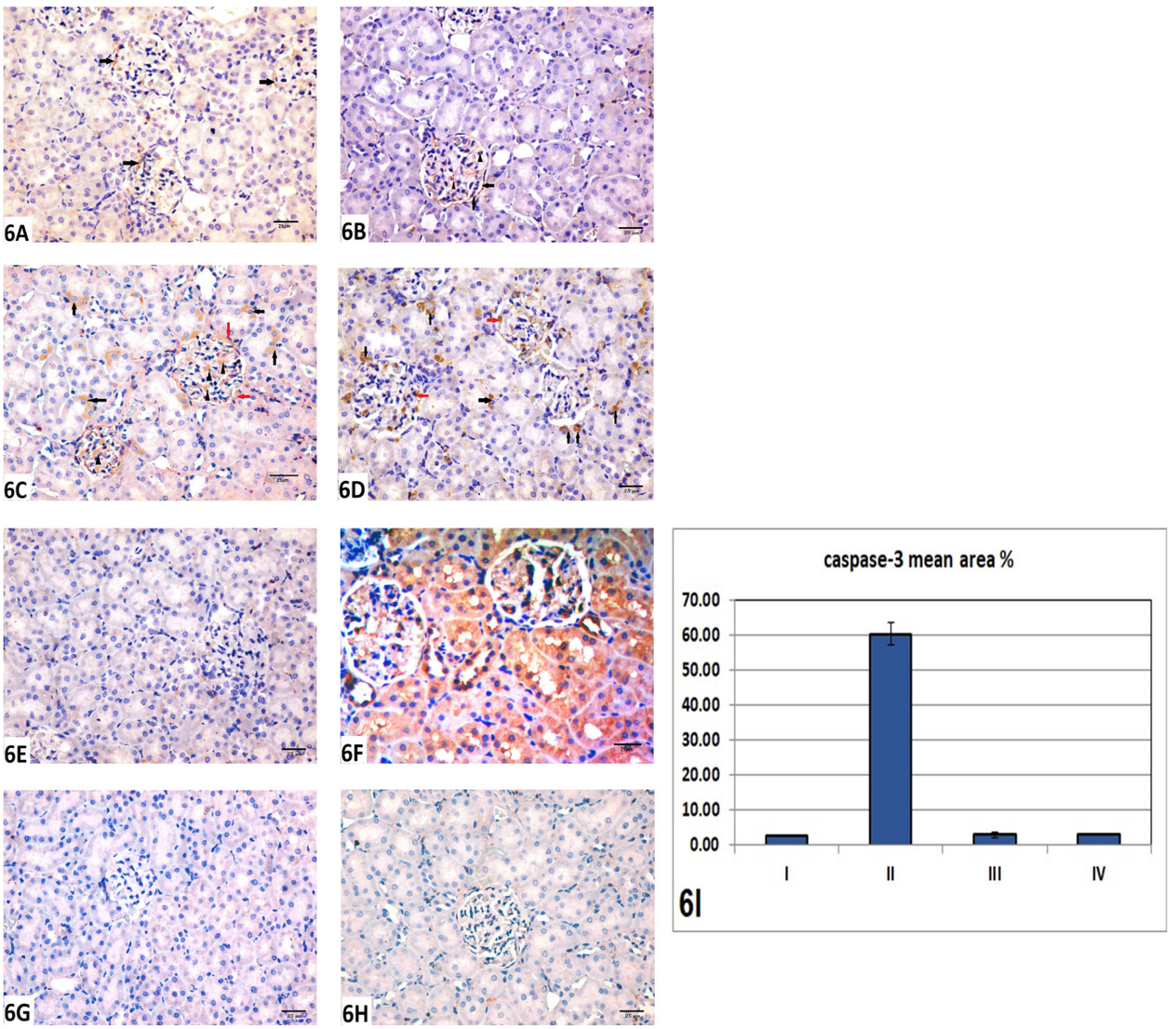

Fig. 6: (A-D): Kidney sections stained with anti-CD34 on day 5 (x400).
(A) Control group (I) getting strong immunoreactivity in endothelial cells (arrow) and no immunoreactive hematopoietic stem cells can be found.
(B) Remdesivir treated group (II) revealing few immunoreactive hematopoietic stem cells identified in glomerular cells; (arrowhead).
(C) BM-MSCs and remdesivir treated group (III) displaying several immunopositive hematopoietic stem cells in renal glomeruli (arrowhead) and tubular epithelium (black arrow). Positive immune responses can also be seen in endothelial cells (red arrow).
(D) G-CSF and remdesivir treated group (IV) containing many immunopositive hematopoietic stem cells in renal glomeruli (arrowhead) and tubular epithelium (black arrow). Positive immune responses can also be seen in endothelial cells (red arrow).
(E-H) Caspase-3 marker expression within sections of the renal cortex(x400):
(E) Control group (I) revealed a negative caspase-3 reaction.
(F) remdesivir treated group (II) demonstrated a strong positive immune-histochemical cytoplasmic reaction within tubular epithelial and a moderate glomerular positive reaction to caspase-3.
(G) BM-MSCs and remdesivir treated group (III) displaying negative cytoplasmic reaction of caspase-3 within the glomerular and tubular epithelium (Fig.).
(H) G-CSF and remdesivir treated group (IV) showing negative cytoplasmic caspase-3 reaction within the glomerular and tubular epithelium
(I) A histogram showing caspase-3 mean area % of immunoreaction.

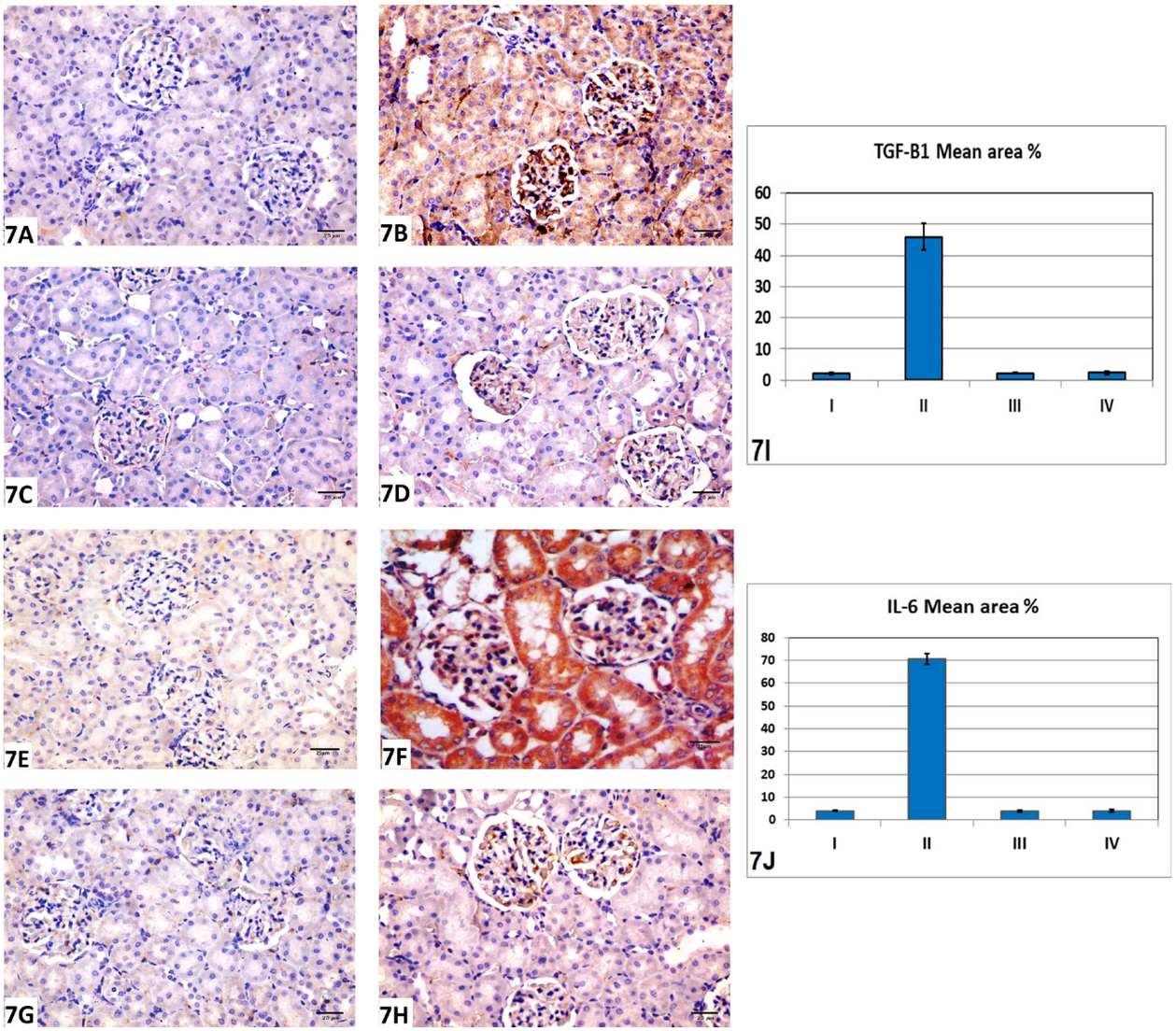

Fig. 7: (A-D) A renal cortex section staine with TGF-β1(x400):
(A) control group (Group I) showing negative immune-histochemical cytoplasmic reaction for TGF-β1 within the glomerular and tubular epithelium.
(B): Remdesivir treated male albino rat (Group II) showing strong positive immune-histochemical cytoplasmic reaction for TGF-β1 within the glomerular and tubular epithelium.
(C): BM-MSCs and remedesivir treated group (III) showing negative immune-histochemical cytoplasmic reaction for TGF-β1 within the glomerular and tubular epithelium.
(D): GCSF and remedesivir-treated group (IV) showing mild positive immune-histochemical cytoplasmic reaction for TGF-β1 within the glomerular epithelium and tubular epithelium.
(E-H) A renal cortex section stain with Il-6 (x400):
(E): control group (I) showing negative immune-histochemical cytoplasmic reaction for IL-6 within the glomerular and tubular epithelium.
(F): Rremdesivir treated male albino rat (Group II) showing a strong positive immune-histochemical cytoplasmic reaction for IL-6 within tubular epithelial and a moderate positive reaction within the glomerular epithelium.
(G): BM-MSCs and remedesivir treated group (III) showing negative immune-histochemical cytoplasmic reaction for IL-6 within the glomerular and tubular epithelium.
(H): GCSF and remedesivir-treated group (IV) showing mild positive immune-histochemical cytoplasmic reaction for IL-6 within the glomerular epithelium and tubular epithelium.
(I) A histogram showing mean area % of TGF-β1 immunreactivity
(J) A histogram showing mean area % of IL-6 immunreactivity

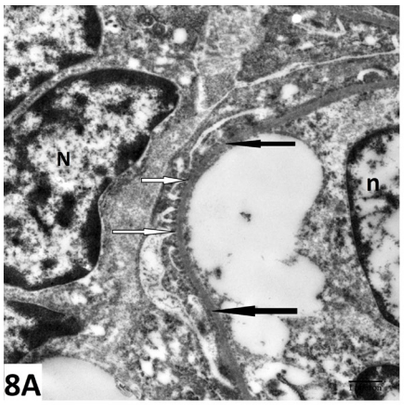

8A

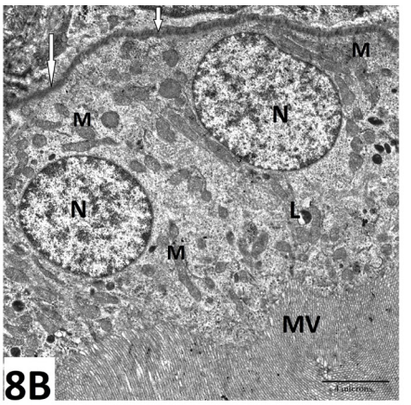

8B

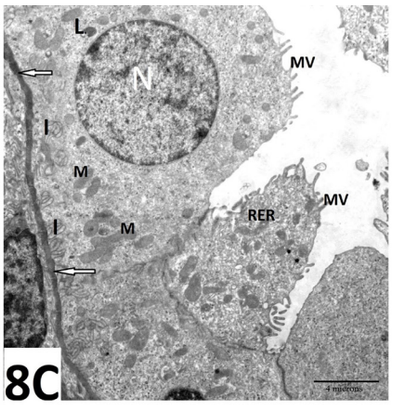

8C

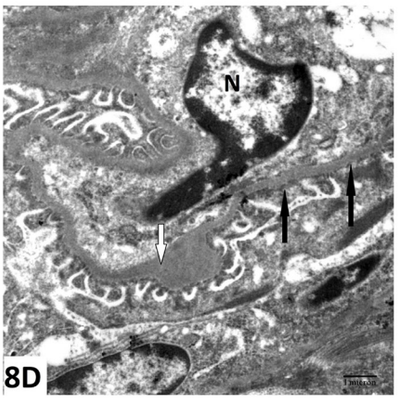

8D

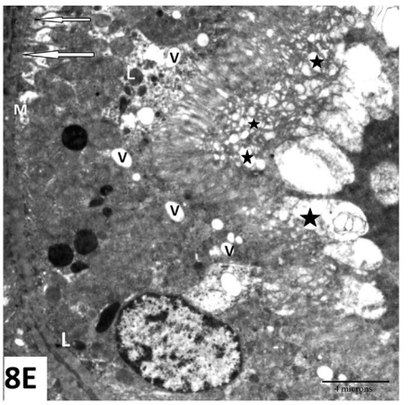

8E

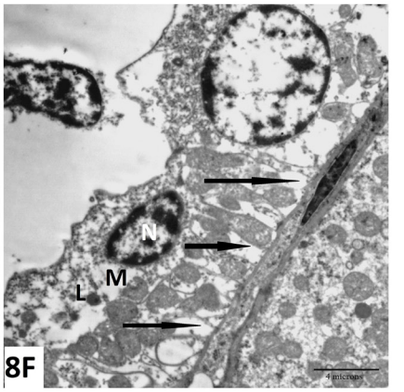

8F

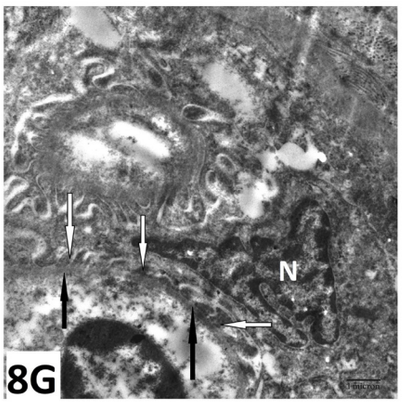

8G

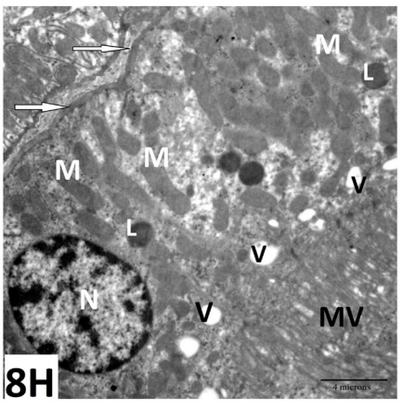

8H

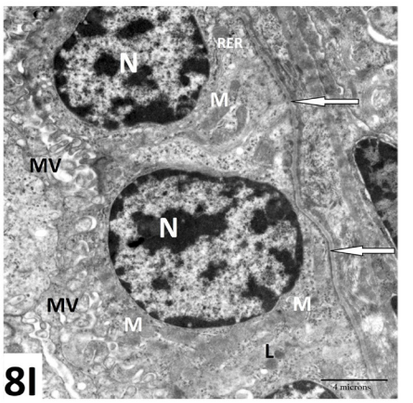

8I

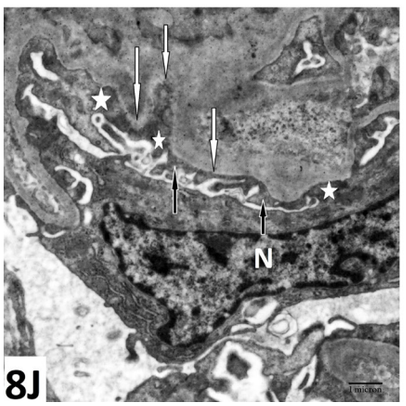

8J

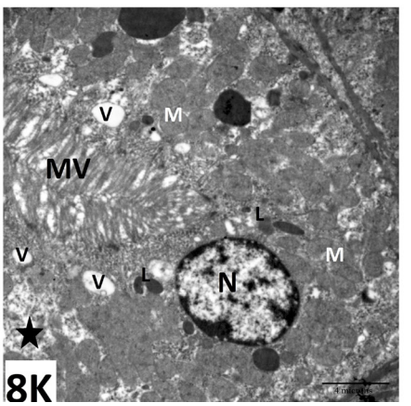

8K

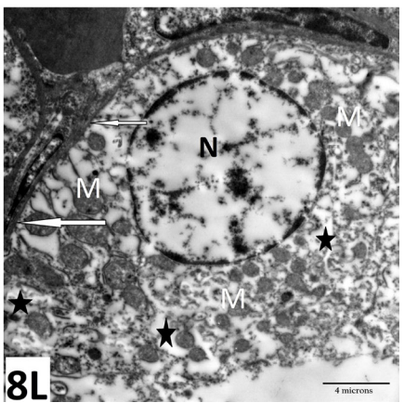

8L

Fig. 8: Transmission electron-micrograph of renal cortex displaying:
(A) Control group (I) showing podocyte with euchromatic nucleus (N) with primary and secondary processes wrapping glomerular capillary. Secondary processes (feet) are separated by filtration slits covered by diaphragm (white arrow). The glomerular capillary has euchromatic nucleus (n) with intact, uniform basement membrane (black arrow). Notice: the glomerular basement membrane is smooth having regular diameter. (TEMx17500)
(B): Control group I showing part of proximal convoluted tubule (PCT) lined with epithelial cells resting on the clear basement membrane (white arrow). PCT cells have central euchromatic nucleus (N). Luminal borders have long slim packed microvilli (MV). Their cytoplasm shows multiple longitudinally oriented mitochondria (M) and lysosomes (L). (TEM×8000)
(C): Group I showing part of distal convoluted tubule (DCT) lined with epithelial cells resting on the clear basement membrane (white arrow). DCT cells have centrally located euchromatic nucleus (N) with apical scarce short microvilli (MV). Their basal membrane shows multiple infolding (I). Their cytoplasm shows multiple longitudinally oriented mitochondria (M), rough endoplasmic reticulum (RER) and lysosomes (L). (TEM×8000)
(D): Remdesivir treated group (II) showing glomerulus with thickening of glomerular capillary basement membrane (white arrow) and podocyte with pyknotic nucleus (N). Fusion and broadening of secondary foot processes (black arrow) of podocyte rested on basement membrane of glomerular capillary is seen with loss of slit diaphragms in-between. (TEM x 17500)
(E): Remdesivir treated group (II) showing part of PCT. Their lining cells have rarified cytoplasm with multiple vacuoles (V) and lysosomes (L). Disturbed luminal surface with multiple vacuoles (black star) is noticed. The basal plasma membrane has dilated infolding (white arrow) having degenerated mitochondria (M). (TEM × 8000)
(F): Remdesivir treated group (II) showing part of DCT. Its lining cell has shrunken heterochromatic nucleus (N). The basal plasma membrane shows dilated infolding (black arrow) with degenerated mitochondria (M) and lysosomes (L), The apical plasma membrane micro-projections are lost. (TEM x 8000)
(G): BM-MSCs and remdesivir treated group (III) showing showing podocyte with indented heterochromatic nucleus (N) with nearly normal secondary processes (feet) (white arrow) wrapping clear thin basement membrane (black arrow) with regular diameter of glomerlular capillary. TEM x17500)
(H): BM-MSCs and remdesivir treated group (III) showing part of proximal convoluted tubule (PCT) lined with epithelial cells with central euchromatic nucleus (N) resting on the clear basement membrane (white arrow). The basal plasma membrane shows multiple infoldings having multiple longitudinally oriented mitochondria (M). Luminal borders have long slim packed microvilli (MV). Their cytoplasm shows lysosomes (L), and few apically located vacuoles (V). (TEM×8000)
(I): BM-MSCs and remdesivir treated group (III) showing part of distal convoluted tubule (DCT) lined with epithelial cells resting on the clear basement membrane (white arrow). The cells have centrally located euchromatic nucleus (N) with apical short microvilli (MV). Their cytoplasm shows multiple longitudinally oriented mitochondria (M), lysosomes (L), Rough endoplasmic reticulum (RER) and free ribosomes. (TEM×8000)
(J): G-CSF and remdesivir treated group (IV) showing podocyte with irregular heterochromatic nucleus (N) having primary and secondary processes (feet) (black arrow) wrapping thin basement membrane with irregular diameter (white arrow). The secondary processes are irregular in shape showing broadening and fusion in many sites (white star). (TEM x17500)
(K): G-CSF and remdesivir treated group (IV)showing part of PCT showing nearly normal lining of epithelial cells having euchromatic nucleus (N). The luminal surface has apical long microvilli (MV). The cytoplasm has numerous mitochondria (M) and lysosomes (L). Notice: focal lytic area (black star) within the cytoplasm and apical vacuoles (V) can be seen. (TEM x 8000)
(L): G-CSF and remdesivir treated group (IV) showing part of DCT. Its lining epithelial cell has central rounded euchromatic nucleus (N). The cytoplasm has nearly normal mitochondria (M). Dilated basal plasma membrane infoldings (white arrow), multiple lytic areas within the cytoplasm (black star) and loss of apical luminal microvilli are still noticed. (TEM x 8000)

Table 1: Effect of different treatments on biochemical and histological parameters in the kidny

	$\bar{X}$±SD				*P-Value*
	I	II	III	I	
Body weight in grams	209.40±7.3	207.20±4.9	204.60±3.2	204.7±3.00	P1= 0.45 P2= 0.1 P3= 0.08
Kidney weight in grams	0.81±0.01	0.96±0.12	0.81±0.017	0.81±0.09	P1= 0.0023 P2= 0.37 P3= 0.09
Plasms creatinine (mmol/L)	0.47±0.03	1.58±0.09	0.53±0.06	0.52±0.11	P1= 0.0001 P2= 0.055 P3= 0.18
Plasma urea (mmol/ L)	29.24±1.03	65.52±5.6	29.96±0.52	30.47±1.74	P1= 0.0001 P2= 0.056 P3= 0.1
GSH (µmol/gm)	6.44±0.46	3.97±0.38	6.63±0.67	6.74±0.15	P1= 0.0001 P2= 0.34 P3= 0.11
MDA (nmol/mg protein)	15.11±0.57	15.13±0.48	15.50±0.76	15.44±0.62	P1= 0.9 P2= 0.17 P3= 0.19
SOD (u/mg protein)	217.80±4.14	159.00±2.61	215.2±5.8	215.10±3.41	P1= 0.0001 P2= 0.4 P3= 0.22
CAT (u/mg protein)	524.00±17.92	351.40±11.36	527.50±19.84	522.30±4.3	P1= 0.0001 P2= 0.84 P3= 0.75
Diameter of renat corpuscle (µm)	123.27±0.45	135.86±10.76	124.35±2.8	123.97±1.35	P1= 0.0001 P2= 0.27 P3= 0.13
Diameter of Bowman's space (µm)	28.19±0.26	42.61±2..42	28.66±0.62	28.69±0.65	P1= 0.0001 P2= 0.1 P3= 0.06
% area of collagen surface area	10.43±0.10	27.25±0.23	10.68±0.35	10.58±0.4	P1= 0.0001 P2= 0.06 P3= 0.28
Caspase immune reactivity	2.79±0.38	60.50±3.27	3.04±0.7	3.09±0.17	P1= 0.0001 P2= 0.17 P3= 0.022
TGF-β1 immune reactivity	2.14±0.22	45.90±4.2	2.21±0. 2	2.37±0.4	P1= 0.0001 P2= 0.41 P3= 0.09
IL-6 immune reactivity	3.99±0.13	70.60±2.22	3.78±0.42	4.08±0.5	P1= 0.0001 P2= 0.15 P3= 0.5

$\bar{X}$= the mean value. SD= the standard deviation.
Significant from the control group (p<0.001).

DISCUSSION

Remdesivir, a novel and promising antiviral treatment, has demonstrated in *vitro* efficacy in corona viruses with certain adverse effects such as acute kidney damage, rash, elevated liver enzymes, and drug intolerance[1,8]. All previous adverse reactions indicated the need to use some type of therapy to mitigate the impact of remdesivir on the kidney, which is why the current research was planned to evaluate and compare the potential ameliorative influence of G-CSF versus BM-MSCs on acute kidney injury caused by a novel antiviral drug.

Mobilization and homing of endogenous hemopoietic stem cells (HSCs) in renal tissue was immunohistochemically tested using CD34 on the 5th day of maximum HSC mobilisation as stated by others[42].

Our data indicated significant increase in kidney weight which indicated renal histo-pathological changes and toxicity as previosouly confirmed[43].

Our findings revealed increased serum urea and creatinine in remdesivir treated animals agreed with others[44,45] who recorded that 27 % of patients treated with remdesivir had high levels of serum creatinine and urea, while 63 % of the subjects surveyed had proteinuria. Therefore, it is critical for patients suffering from pre-existing renal dysfunction or undergoing multidrug therapy to monitor renal function during remdesivir therapy according to the safety profile of the remdesivir antiviral drug[46]. A reduction in glomerular filtration rate (GFR) and a decrease in creatinine clearance may occur due to the adverse effect of remdesivir on the kidney according to authorised fact sheet for health care providers in EMERGENCY USE AUTHORIZATION (EUA) OF VEKLURY®[47]. Remdeivir is not approved for adult patients with a decreased glomerular filtration rate[48]. A significant decrease in reduced glutathione (GSH), superoxide dismutase (SOD) and catalase (CAT) enzymes was induced by Remdesivir. Remdesivir metabolite is an efficient substrate of rat organic anion transporter 3 (OAT3) and exhibits OAT3-dependent cytotoxicity in rats[49]. Rat OAT3 can transport GSH to the kidney[50]. GSH is passed to the renal proximal tubule via both sodium-coupled and sodium-independent pathways through the basolateral plasma membrane (BLM). GSH presents in the mitochondria with abundance in the matrix[51]. Intracellular GSH plays a crucial role in the maintenance of cell viability and mitochondrial function[52]. Mitochondrial dysfunction can trigger the release of ROS[53].

In the remdesivir-treated group, significant renal cortex histology disruption was identified in the form of swollen, fragmented and degenerated renal glomeruli with renal interstitium degeneration and wide spaces. In addition, dilated renal tubules having acidophilic casting within their lumen tended to be distorted, with the involvement of their epithelial lining having nuclei with varying degrees of degeneration (pyknosis and karyolysis). Both of the above results revealed renal injury. The same results were consistent with the European Medicines Agency[49] that observed renal tubular atrophy, casting, and increased mean urea nitrogen and serum creatinine following intravenous administration of remdesivir at different doses to male rhesus monkeys. Herlitz *et al*. reported that nucleoside analogues prodrug induced tubule-interstitial change as tubular atrophy and interstitial fibrosis[54].

Treatment with remdesivir caused glomerular capillary vacuolations lined with darkly stained small pyknotic nuclei. Congested glomeruli and perintubular capillaries, widening of Bowman's space with parietal layer disruption, were observed. These results were suggestive of renal injury and dysfunction as reported in a fact sheet for health care provider EMERGENCY USE AUTHORIZATION (EUA) OF VEKLURY[47], after 4 weeks of intravenous injection of remdesiver to rats. Accumulation of triphosphate metabolites of the drug led to tubular degeneration which was accompanied by congestion of glomerular capillaries, widening of the glomerular capsular space. Some tubules lumens showed traces of degenerated cells[54]. In addition, researchers[8] reported haematuria, kidney injury and renal tubular atrophy in 4 %, 6 percent and 8 % respectively after remdesivir in covid 19 patients. Additionally, acute renal failure was reported in randomised controlled trials performed in Wuhan, China in 2020 in covid 19 patients treated with remdesivir[6]. Renal tubular vacuolation due to the accumulation of remdesivir carrier sulfobutyl ether-beta-cyclodextrin (SBECD) were recorded[55]. Others[56] recorded that 23 % of patients receiving remdesivir had renal dysfunction. Ingrahamet *et al*,[57] also reported that remdsevir caused acute renal injury.

Microscopic evaluation of the renal section of remdesivir treated rat stained with Mallory trichrome (MT) showed a substantial marked accumulation of collagen fibres in the interstitium and between glomerular capillaries in the renal cortex compared to the control group. This was confirmed by a morphometric study showing that the mean area percent of collagen fibres was significantly higher than the control. This may be described as a reaction to renal tubular and interstitial injury resulting in inflammation and fibrosis[58]. Excessive deposition of collagen in the extracellular matrix was linked to interstitial fibroblasts responsible for excess ECM and impaired collagen synthesising epithelial cells manifested as both basement membrane thickening and interstitial fibrosis[59].

Also, Gewin *et al*.,[60] justified the occurrence of renal fibrosis due to the development of many profibrotic factors such as TGF-β and TGF-β/Smad3 signal pathways. Degeneration and loss of renal tubules contribute to interstitial fibrosis and TGF-β1[61]. This was recorded in the present study by demonstrating a strong positive immune-histochemical cytoplasmic response to TGF-β1 within the glomerular and tubular epithelium.

Caspase-3 expression has been significantly enhanced in the remdesivir-treated group. This can be due to SBECD, which has been shown to cause human renal cell line apoptosis[62].

Interleukin-6 (IL6) is a multifunctional cytokine responsible for controlling various biological processes such as organogenesis, immune responses, IgG production, inflammation, and acute phase reactions[63]. IL6 expression is a complex and contentious process. In this assessment, remdesivir induced IL-6 expression in renal cortex, as demonstrated by a strong positive immune-histochemical cytoplasmic reaction to the epithelial tubular and a moderate glomerular positive reaction to IL6. Our results were consistent with recent studies that associated acute kidney injury with IL6 expression. Local and systemic increase in IL-6 signaling and transcription following bilateral renal ischemia was recorded for 60 minutes in acute ischemic kidney injury using the animal model. Therefore, IL-6 signaling was also specifically linked to systemic and local inflammation and can be used as a biomarker as well as a therapeutic predictor for ischemic renal disease[64]. In addition, acute kidney injury due to nephrotoxin had increased renal IL-6 expression and was intensely associated with kidney damage. Additionally, IL-6 mediated neutrophil activation among the key pathways involved in acute kidney injury and thus neutrophil depletion in mice minimized renal nephrotoxin induced injury[65].

Electron microscopic findings showed glomerular basement membrane thickening, vacuolation of the renal tubules and degenerated mitochondria. Our results were in line with Charan *et al*.[66] who stated that remdesivir induced renal dysfunction and decreased glomerular filtration rates. The reduction in GFR may be due to thickening of the glomerular basement membrane. Luk *et al*.,[55] recorded acute renal tubular vacuolation. Hewitson *et al*.,[59] demonstrated basement membrane thickening due to injury to epithelial cells. Animal studies documented accumulation of sulfobutylether-β-cyclodextrin (SBECD) when using remdesivir leading to obstruction of renal tubules[11]. Adamsick *et al*.[7] identified remdesivir triphosphate metabolites with long half-life plasma mediated mitochondrial toxicity. Mitochondrial degeneration is an early stage of cell death. Mitochondria play a vital role in active transport, which needs high energy[67]. Fusion and broadening of secondary foot processes and loss of slit diaphragms may be rendered to mitochondrial toxicity[68]. Disturbed luminal surface and dilated basal plasma membrane in-folding with degenerated mitochondria were recorded by others[69] who found thinning of the brush-border, tubular cell swelling and cell necrosis in nucleosides analogues prodrugs.

BM-MSCs are multipotent mesenchymal stromal cells known as self-renewing cells present in all postnatal tissues and organs[70] Animal treated with remdesivir concomitantly with BM-MSCs showed normal serum urea and creatinine, normal levels of SGH, SOD and CAT. Histological finings revealed renal structure as normal renal glomeruli appeared surrounded by normal Bowman capsule, normal renal tubules, and interstitium. Our results coincided with that of others[71] who documented that intravenous administration of MSCs in small animals had a therapeutic effect on renal injury. MSCs decreased serum urea and creatinine, oxidative stress markers, apoptosis and collagen deposition, and increased tubular proliferation. In this study, caspase-3, IL-6 and TGF-β1 were significantly reduced, as reported by Wang *et al*.,[71] who also, indicated that MSCs reduced IL-6 and TGF-β1 expressions. MSCs increased acute renal disruption minimized apoptosis and inhibited oxidative stress[72]. The homing of MSCs to the injured tissues was triggered by a number of chemokine releases from the wounded tissue and chemokine receptors expressed by MSCs. The healing effects of MSCs were derived primarily from their penetration in the injured kidney and the resulting trans-differentiation of MSCs to kidney-specific cells to model the kidney[73].

G-CSF and the remdesivir-treated group showed normal serum urea and creatinine and normal levels of SGH, SOD and CAT. Histological finings revealed nearly normal renal architecture. This was confirmed by others[30]. who stated that G-CSF improved mobilization of endogenous hemopoietic stem cells (HSCs), so restored normal renal structure and reduced renal injury and development of reactive oxygen species (ROS) and levels of urea and creatinine. Mobilization of HSCs and G-CSF endothelial progenitor cells to injured renal tissue were responsible for the healing effect[74]. Previous studies also demonstrated that G-CSF induced angiogenesis in myocardial infarction, cerebral ischemia, and limb ischemia, which facilitates the tissue regeneration of injured cells[75]. Reduction in renal fibrosis was confirmed by Fang *et al*.[76] who found that G-CSF treatment significantly decreased collagen deposition in mice treated with carbon dichloride and pentachloride. G-CSF developed anti-fibrogenic cytokines[77] and reduced TGF-β1 expression and therefore reduced collagen deposition[78] as demonstrated in our study. G-CSF reduced TGF-b1, collagen type IV, and IL-6 mRNA[79].

CONCLUSION

Administering drugs such as remdesivir should also proceed with strict caution. The current research is promising for impaired renal function. Both BM-MSCs and G-CSF boost histological structure, ultrastructure and kidney function. G-CSF is a hopeful prospect for the treatment of kidney injury. G-CSF is an efficient and perfect option to protect the patient from permanent kidney damage.

CONFLICT OF INTERESTS

There are no conflicts of interest.

REFERENCES

1. Antinori, S., Cossu, M., Ridolfo, A., Rech, R., Bonazzetti, C., Pagani, G., Gubertini, G., Coen, M., Magni, C., Castelli, A., *et al*., (2020): “Compassionate remdesivir treatment of severe Covid-19 pneumonia in intensive care unit (ICU) and non-ICU patients: Clinical outcome and differences in post-treatment hospitalization status. Pharmacological Research 158. 104899.

2. Bose, S., Adapa, S., Aeddula, N., Roy, S., Nandikanti, D., Vupadhyayula, P., Naramala, S., Gayam, V., Muppidi, V and Konala, V., (2020): "Medical management of CVID19: Evidence and experience". Elmer Press. J. Clin. Med. Res.; 12(6):329-343.

3. Sheahan, T., Sims, A., Graham, R., Menachery, V., Gralinski, L., (2017): "Broad-spectrum antiviral GS-5734 inhibits both epidemic and zoonotic coronaviruses". Sci, Transl. Med.9: eaal3653.

4. Agostini, M., Andres, E., and Sims, A., (2018): "Coronavirus susceptibility to the antiviral remdesivir (GS-5734) is mediated by the viral polymerase and the proofreading exoribonuclease". mBio 9: e00221-18.

5. Al-Tawfiq, J., AL-Homoud, A., and Memish., Z. (2020): "Remdesivir as a possible therapeutic option for the COVID-19". Travel Med. Infect. Dis. 34. 101615.

6. Wang, Y., Zhang, D., Du, G., Du, R., Zhao, J., Jin, Y., *et al*. (2020): "Remdesivir in adults with severe COVID-19: a randomised, double-blind, placebo-controlled, multi-center trial". Lancet. 395 (10236): 1569–1578.

7. Adamsick, M., Gandhi, R., Bidell, M., Elshaboury, R., Bhattacharyya, R., Kim, A., Rhee, E and Sise, M., (2020):" Remdesivir in patients with acute or chronic kidney disease and COVID-19". The American Society of Nephrology. 31: 1384-1386. ISSN: 1046-6673/3107-1384.

8. Grein, J., Ohmagari, N., Shi, D., *et al*., (2020): "Compassionate use of remdesivir for patients with severe Covid-19". N. Engl. J. Med. 382: e101.

9. Hillaker, E., Belfer, J., Bondici, A., Murad, h., and Dumkow, L., (2020): "Delayed initiation of remdesivir in a COVID-19 positive patient". Pharmacotherapy. 40(6):592-598.

10. Ko, W., Rolain, J., Lee, N., *et al*., (2020): "Arguments in favour of remdesivir for treating SARS-CoV-2 infections". Int. J. Anti-microb. Agents 55 (4):105933.

11. Kiser, T., Fish, D., Aquilante, C, Rower, J., Wempe, M., MacLaren, R. *et al*., (2015): "Evaluation of sulfobutylether- β - cyclodextrin (SBECD) accumulation and voriconazole pharmacokinetics in critically ill patients undergoing continuous renal transplant therapy". Crit. Care. 19(1):32.

12. Miettinen, J., Salonen, R., Ylitalo, K., *et al*. (2012): "The effect of bone marrow microenvironment on the functional properties of the therapeutic bone marrow-derived cells in patients with acute myocardial infarction". J. Transl. Med. 10:1–11.

13. Horwitz, E., Le-Blanc, K., Dominici, M., *et al*., (2005): "Clarification of the nomenclature for MSC: the international society for cellular therapy position statement". Cytotherapy. 7:393-395.

14. Parekkadan, B., and Milwid, J., (2010): "Mesenchymal stem cells as therapeutics". Annual Review of Biomedical Engineering. 12: 87–117.

15. Papazova, A., Oosterhuis, R., Gremmels, H., van Koppen, A., Joles, J., Verhaar, M., (2015): "Cell-based therapies for experimental chronic kidney disease: A systematic review and meta-analysis". Dis. Model. Mech. 8: 281–293.

16. Galipeau, J., and Sensebe, L., (2018): "Mesenchymal Stromal Cells: Clinical Challenges and Therapeutic Opportunities". Cell Stem Cell. 22: 824–833.

17. Yadav, N., Rao, S., Bhowmik, D., and Mukhopadhyay, A., (2012): "Bone marrow cells contribute to tubular epithelium regeneration following acute kidney injury induced by mercuric chloride". Indian J. Med. Res. 136:211-220.

18. Morigi, M., Introna, M., Imberti, B., (2008): "Human bone marrow mesenchymal stem cells accelerate recovery of acute renal injury and prolong survival in mice". Stem Cells. 26:2075-2082.

19. Yen, T., Alison, M., Cook, H., *et al*., (2007): "The cellular origin and proliferative status of regenerating renal parenchyma after mercuric chloride damage and erythropoietin treatment". Cell Proliferation. 40 (2): 143–156.

20. Bi, B., Schmitt, R., Israilova, M., Nishio, H., and Cantley, L., (2007): "Stromal cells protect against acute tubular injury via an endocrine effect". J. Am. Soc. Nephrol. 18:2486-2496.

21. Wise, A., and Ricardo, S., (2012): "Mesenchymal stem cells in kidney inflammation and repair". Nephrology. 17(1):1-10.

22. Humphreys, B., and Bonventre, J., (2008): "Mesenchymal stem cells in acute kidney injury". Annual Review of Medicine. 59: 311–325.

23. Magen, D., Mandel, H., Berant, M., Ben-Izhak, O., and Zelikovic, I., (2002): "MPGN type I induced by granulocyte colony stimulating factor". Pediatr Nephrol. 17:370–2.

24. Zohlnhofer, D., Ott, I., Mehilli, J., Schomig, K., Michalk, F., Ibrahim, T., Meisetschlager, G., Wedel, J., Bollwein, H., Seyfarth, M., Dirschinger, J., Schmitt, C., Schwaiger, M., Kastrati, A., and Schomig, A., (2006): "Stem cell mobilization by granulocyte colony stimulating factor in patients with acute myocardial infarction: a randomized controlled trial". JAMA; 295: 1003–1010.

25. Nishida, M., Fujimoto, S., Toiyama, K., Sato, H., Hamaoka, K., (2004):" Effect of hematopoietic cytokines on renal function in cisplatin induced ARF in mice". Biochem. Biophys. Res. Commun. 324: 341–347.

26. Stokman, G., Leemans, J., Claessen, N., Weening, J., and Florquin, S., (2005): "Hematopoietic stem cell mobilization therapy accelerates recovery of renal function independent of stem cell contribution". J Am Soc Nephrol 16: 1684–1692.
27. Deotare, U., Al-Dawsari, G., Couban, S., and Lipton, J., (2015):" G-CSF-primed bone marrow as a source of stem cells for allografting: revisiting the concept". Bone Marrow Transplant. 50:1150–6.
28. Ito, S., Uchida, T., Oshima, N., Oda, T., and Kumagai, H., (2018): "Development of membrano-proliferative glomerulonephritis-like glomerulopathy in a patient with neutophilia resulting from endogenous granulocyte-cololny stimulating factor overproduction: a case report". BMC Nephrology.19:251; 1-5.
29. Hamed, G.M., Morsy, W.E., Hamid, M.S.A., Hassan, A.A.E.M., Zahra, F.A.A. (2019):" Effect of Bone Marrow-Derived Mesenchymal Stem Cells on Ischaemic-Reperfused Hearts in Adult Rats with Established Chronic Kidney Disease". Int. J. Stem Cells.12(2):304-314.
30. Sadek, E.M., Salama, N.M., Ismail, D.I., Elshafei, A.A. (2016):" Histological study on the protective effect of endogenous stem-cell mobilization in Adriamycin-induced chronic nephropathy in rats". J Microsc Ultrastruct.; 4:133–42.
31. Thakare, S., Gandhi, C., Modi, T., Bose, S., Deb, S., Saxena, N., Katyal, A., Patil, A., Patil, S., Pajai, A., Bajpai, D. and Jamale, T. (2021):" Safety of Remdesivir in Patients with Acute Kidney Injury or CKD". Kidney Int Rep. 6(1): 206–210.
32. Shin, J.W., Seol, I.C. and Son, C.G., (2010): "Interpretation of animal dose and human equivalent dose for drug development. J Korean Orient Med. 31, 1–7.
33. Anderson M. E. (1985): "Determination of glutathione and glutathione disulfide in biological samples". Methods in Enzymology. 113: 548–555.
34. Jurczuk, M., Brzóska, M.M., Moniuszko-Jakoniuk, J., Gałazyn-Sidorczuk, M., Kulikowska-Karpińska, E. (2004):" Antioxidant enzymes activity and lipid peroxidation in liver and kidney of rats exposed to cadmium and ethanol". Food Chem Toxicol.42(3):429-38.
35. Bancroft, J.D. and Gamble, M., (2008):" Theory and practice of histological techniques". sixth edition. Churchill Livingstone, Elsevier, Philadelphia. pp. 126: 150-440.
36. Bancroft, J. and Cook, H. (1994):" Immunocytochemistry. Manual of histological techniques and their diagnostic applications. 2nd ed Edinburgh/London/Madrid/Melbourne/New York/ Tokyo: Churchill Livingstone. p. 263–325.
37. Hong, S. W., Isono, M., Chen, S., Iglesias-De La Cruz, M. C., Han, D. C., and Ziyadeh, F. N. (2001):"Increased glomerular and tubular expression of transforming growth factor-beta1, its type II receptor, and activation of the Smad signaling pathway in the db/db mouse. The American journal of pathology. 158(5): 1653–1663.
38. Kabiraj, A., Gupta, J., Khaitan, T. and Bhattacharya, P., (2015):" Principle and techniques of immunohistochemistry- A review". Int. J. Biol. Med. Res. 6 (3): 5204–5210.
39. Suker, D., AL- Badran, A., Abbas, E., and Abdullah, S., (2017):" Immunohistochemistry Analysis for Interleukin-6 Expression from the Tumor Tissue". International Journal of Science. 3(03).
40. Glauert, A.M. and Lewis, P.R. (1999): "Biological specimen preparation for transmission electron microscope. 1st ed. London: Princeton University Press.
41. Dawson, B. and Trapp, R., (2004):" Basic & Clinical Biostatistics. fourth edition. Lange Med-ical Books – McGraw-Hill, New York, pp. 161–218.
42. Waller, C.F., Bronchud, M., Mair, S.,and Challand, R. (2010):" Comparison of thepharmacodynamic profiles of a biosimilar filgrastim and Amgenfilgrastim: results from a randomized, phase I trial. Ann Hematol.; 89: 971–8.
43. Craig, E.A., Yan, Z.,and Zhao QJ. (2015):"The relationship between chemical-induced kidney weight increases and kidney histopathology in rats. J Appl Toxicol.";35(7):729-36.
44. Diao, B., Wang, C., Wang, R., Feng, Z., Tan, Y., Wang, H., *et al*. (2020):" Human kidney is a target for novel severe acute respiratory syndrome coronavirus 2(SARS-CoV-2) infection". medRxiv.2020:2020.03.04.20031120.
45. Li Z, Wu M, Guo J, Yao J, Liao X, Song S, *et al*. (2020):" Caution on Kidney Dysfunctions of 2019-nCoV Patients". medRxiv. 2020:2020.02.08.20021212.
46. Safety profile of the antiviral drug remdesivir: An update, (2020): Biomedicine and Pharmacotherapy.130.110532.
47. US Food and Drug Administration: Fact Sheet for Health Care Providers Emergency Use Authorization (EUA) of Remdesivir (GS-5734 TM), Silver Spring, MD, US Food and Drug Administration, 2020.
48. Sanders, J., Monogue, M., Jodlowski T., Cutrell J., (2020): "Pharmacologic treatments for coronavirus disease 2019 (COVID-19): A Review". JAMA.
49. European Medicines Agency (2020):" Summary on compassionate use Remdesivir Gilead: http:// www.ema.europa.eu/en/documents/other/summary compassionate-use-remdesivir-gilead_en.pdf.

50. Lash, L. H., Putt, D. A., Xu F., and Matherly L. H. (2007):" Role of rat organic anion transporter 3 (Oat3) in the renal basolateral transport of glutathione. Chemico-Biological Interactions". 2007;170(2):124–134.

51. Mari M. Colell A. Morales A. von Montfort C. Garcia-Ruiz C. Fernandez-Checa J. C. (2010):" Redox control of liver function in health and disease. Antioxid. Redox Signal". 12 1295–1331.

52. Lash L. H. (2006):" Mitochondrial glutathione transport: physiological, pathological, and toxicological implications". Chem. Biol. Interact. 163 54–67.

53. Srinivasan, S. and Avadhani, N.G. (2012):" Cytochrome C oxidase dysfunction in oxidative stress. Free Radic Biol Med.15;53(6):1252-63.

54. Herlitz LC, Mohan S, Stokes MB, Radhakrishnan J, D'Agati VD, Markowitz GS.(2010): " Tenofovir nephrotoxicity: acute tubular necrosis with distinctive clinical, pathological, and mitochondrial abnormalities. Kidney International. 78(11):1171–1177.

55. Luke, D., Tomaszewski, K. Bharat Damle, B., and Schlamm, H.T. (2010): "Review of the basic and clinical pharmacology of sulfobutylether β- cyclodextrin". J Pharm Sci. 2010 Aug; 99(8):3291-301.

56. Jorgensen, S.C.J., Kebriaei, R. and Dresser, L.D. (2020):" Remdesivir: Review of Pharmacology, Pre-clinical Data, and Emerging Clinical Experience for COVID-19". Pharmacotherapy. 40(7):659-671.

57. Ingraham, N.E., Barakat, A.G., Reilkoff, R., Bezdicek, T., Schacker, T., Chipman, J.G., *et al*. (2020):" Understanding the renin-angiotensin-aldosterone-SARS-CoV-axis: A comprehensive review. Eur Respir J. 2020:2000912.

58. Black, L.M., Lever, J.M., Agarwal, A. (2019):" Renal Inflammation and Fibrosis: A Double-edged Sword". Journal of Histochemistry & Cytochemistry. 2019;67(9):663-681.

59. Hewitson, T.D., Holt, S.G., and Smith, E.R. (2017): "Progression of Tubulointerstitial Fibrosis and the Chronic Kidney Disease Phenotype - Role of Risk Factors and Epigenetics". Front Pharmacol.;8: 520.12.

60. Gewin, L., Zent, R., and Pozzi, A., (2017): "Progression of chronic kidney disease: too much cellular talk causes damage". Kidney Int.;91(3):552-60.

61. Liu, B.C., Tang, T.T., Lv, L.L., and Lan, H.Y. (2018):" Renal tubule injury: a driving force toward chronic kidney disease. Kidney Int. 2018;93(3):568-79.

62. Rowe ES, Rowe VD, Biswas S, Mosher G, Insisienmay L, Ozias MK, Gralinski MR, Hunter J, Barnett JS. (2016):" Preclinical Studies of a Kidney Safe Iodinated Contrast Agent". J Neuroimaging. 2016 Sep;26(5):511-8.

63. Su, H., Lei, C-T and Zhang, C. (2017): "Interleukin-6 Signaling Pathway and Its Role in Kidney Disease: An Update". The journal Frontiers in Immunology. Vol. 8: 405: 1-10. doi: 10.3389/.

64. Grigoryev, D., Liu, M., Hassoun, H., Cheadle, C., Barnes, K., and Rabb, H., (2008): "The local and systemic inflammatory transcriptome after acute kidney injury". J. Am. Soc. Nephrol. 19: 547-58.

65. Nechemia-Arbely, Y., Barkan, D., Pizov, G., Shriki, A., Rose-John, S., Galun, E., *et al*., (2008): "IL-6/IL-6R axis plays a critical role in acute kidney injury". J. Am. Soc. Nephril. 19: 1106-15.

66. Charan, J., Kaur, R.J., Bhardwaj, P., Mainul-Haque, D, Sharma, P.E., Misraf, S. and Godman, B. (2020):" Rapid review of suspected adverse drug events due to remdesivir in the WHO database; findings and implications". Expert Rev Clin Pharmacol. doi:10.1080/17512433.2021.1856655.

67. Perico L, Morigi M, Rota C, Breno M, Mele C, Noris M, Introna M, Capelli C, Longaretti L, Rottoli D, Conti S, Corna D, Remuzzi G, Benigni A, (2017): "Human mesenchymal stromal cells transplanted into mice stimulates re-nal tubular cells and enhance mitochondrial function". Nat Commun.; 8:983.

68. Gujarati NA, Vasquez JM, Bogenhagen DF, Mallipattu SK. (2020):" The complicated role of mitochondria in the podocyte. Am J Physiol Renal Physiol. Dec 1;319(6):F955-F965.

69. George, N., Basu, G., Mohapatra, A., Zachariah, U., Abraham, P., Korula, A., Varughese, S., Jacob, C. K., & Tamilarasi, V. (2015): " Adefovir nephrotoxicity in a renal allograft recipient. Indian journal of nephrology, 25(3), 180–183.

70. Porada, D., Zanjani, D., and Almeida-Porad, G., (2006):" Adult mesenchymal stem cells: a pluripotent population with multiple applications". Current stem cell research e-therapy, vol.1, no.3: 365-369.

71. Wang Y, He J, Pei X, Zhao W. (2013):" Systematic review and meta-analysis of mesenchymal stem/ stromal cells therapy for impaired renal function in small animal models". Nephrology (Carlton); 18:201-208.

72. Zhou T, Liao C, Lin S, Lin W, Zhong H, Huang S. (2020):" The Efficacy of Mesenchymal Stem Cells in Therapy of Acute Kidney Injury Induced by Ischemia-Reperfusion in Animal Models". Stem Cells Int.; 2020:1873921.

73. Liu, D., Cheng, F., Pan, S. Liu, Z. (2020):" Stem cells: a potential treatment option for kidney diseases". Stem Cell Res. Ther. 11, 249 (2020).

74. Zhang, J.J., Yi, Z.W., Dang, X.Q., He, X.J. and Wu, X.C. (2007):" Mobilization effects of SCFalong with G-CSF on bone marrow stem cells and endothelial

pro-genitor cells in rats with unilateral ureteral obstruction". ZhongguoDang Dai. Er. Ke. Za. Zhi.; 9:144–8.

75. Ohki, Y., Heissig, B., Sato, Y., Akiyama, H., Zhu, Z., Hicklin, D.J., Shimada, K., Ogawa, H., Daida, H., Hattori, K. and Ohsaka, A. (2005): "Granulocyte colony-stimulating factor promotes neovascularization by releasing vascular endothelial growth factor from neutrophils". FASEB. J.; 19: 2005–2007.
76. Fang B, Luo S, Song Y, Li N, Li H, Zhao R. (2010):" Intermittent dosing of G-CSF to ameliorate carbon tetrachloride-induced kidney fibrosis in mice". Toxicology; 270:43–8.
77. Tilg H, Jalan R, Kaser A, Davies NA, Offner FA, Hodges SJ, *et al*. (2003):" Anti-tumor necrosis factor alpha monoclonal antibody therapy in severealcoholic hepatitis. J. Hepatol.; 38:419–25.
78. Li, N., Zhang, L., Li, H. and Fang, B. (2010):" Administration of granulocyte colony-stimulating factor ameliorates radiation-induced hepatic fibrosis in mice". Transplant Proc.; 42:3833–9.
79. So, B. I., Song, Y. S., Fang, C. H., Park, J. Y., Lee, Y., Shin, J. H., Kim, H., & Kim, K. S. (2013):" G-CSF prevents progression of diabetic nephropathy in rat". PlOS. one, 8(10), e77048.

الملخص العربى

تأثيرعقار الرامدسيفير على الكلى والقدرة الوقائية المحتملة للعامل المحفزلمستعمرة الخلايا المحببة G-CSF مقابل الخلايا الجذعية الوسيطة للنخاع العظمي في ذكور الجرذان البيضاء البالغة

هالة محمد الحرون[١] – منار على بشندى[٢] – منى عبد المولى سليمان[١]

[١]قسم الأنسجة - كلية الطب - جامعة المنوفية

[٢]قسم التشريح والأجنة - كلية الطب - جامعة المنوفية

الخلفيه : الرامدسيفير هو عقار جديد مضاد للفيروسات واسع المجال استخدم سابقًا لعلاج الايبولا. وهو تركيبة للدواء بها نيوكليوسيد و له نشاط مضاد للفيروسات السارس- CoV-٢ والفيروس التاجي.

الهدف: تم التخطيط للبحث الحالي لتقييم ومقارنة التأثير الوقائى المحتمل للخلايا الجذعية المكونة للدم التي يتم حشدها بواسطة العامل المحفز لمستعمرة الخلايا المحببة مقابل الخلايا الجذعية الوسيطة للنخاع العظمي على تأثير مضاد الفيروسات الجديد الرامدسيفير على الكلى.

المواد و الطرق المستخدمة: تم تقسيم الجرذان إلى أربع مجموعات: مجموعة التحكم (الضابطة) ، المجموعة المعالجة بـالرامدسيفير (٢٠ مجم / كجم / يوم بالحقن الوريدى في اليوم الأول يليها ١٠ مجم / كجم / يوم لمدة ٦ أيام) ، مجموعة الرامدسيفير + الخلايا الجذعية الوسيطة للنخاع العظمي (٣ × ١٠ ٦ خليه/ مللى من الخلايا الجذعية الوسيطة المسمى PKH26 ، مجموعة الرامدسيفير + فيلجراستيم (٧٠ ميكروجرام / كجم /يوم لمدة خمسة ايام). و فى نهاية التجربة تم تخدير الحيوانات و ذبحهم . تم استئصال كليتي الحيوان لعمل دراسات نسيجية و كيميائية مناعية وبالمجهر الإلكتروني. كما تم إجراء تقييمات بيوكيميائية و شكلية مورفومترية.

النتائج: تسبب الرامدسيفير في حدوث تشويه وتنكس في كل من الكبيبات والأنابيب الكلوية مع اتساع فضاء بومان. لقد زاد بشكل كبير من ترسب الكولاجين وعزز التعبير عن كاسباس ٣ و انترلوكين ٦ و عامل النمو المحول١β. لوحظت تغييرات في البنية التحتية الدقيقه في شكل سماكة الغشاء القاعدي الكبيبي ، وتوسع غشاء البلازما القاعدي المتوسع للظهارة الأنبوبية وتنكس الميتوكوندريا. كيميائيا ، تم تسجيل انخفاض فى إنزيمات مضادات الأكسدة ، انخفاض الجلوتاثيون (GSH) ، ديسموتاز الفائق (SOD) ، والكتلاز (CAT) مع زيادة اليوريا والكرياتينين في الدم. سجل كل من الخلايا الجذعية الوسيطة للنخاع العظمي و العامل المحفزلمستعمرة الخلايا المحببة تحسن فى البنية النسيجية ووظيفة الكلى.

الاستنتاج: يجب أن يتم وصف الأدوية مثل الرامدسيفير بعناية شديدة. الخلايا الجذعية الوسيطة للنخاع العظمي و العامل المحفز لمستعمرة الخلايا المحببة هي خيار فعال ومثالي لحماية المرضى من تلف الكلى الدائم.